ACS APPLIED MATERIALS & INTERFACES

Research Article

www.acsami.org

Conducting Polymer Transistors Making Use of Activated Carbon Gate Electrodes

Hao Tang,[†,⊥] Prajwal Kumar,[†,⊥] Shiming Zhang,[†,⊥] Zhihui Yi,[†] Gregory De Crescenzo,[†] Clara Santato,[‡] Francesca Soavi,[§] and Fabio Cicoira*[,†]

[†]Department of Chemical Engineering, Polytechnique Montreal, C.P. 6079, Succ. Centre Ville, Montreal H3C 3A7, Canada

[‡]Department of Engineering Physics, Polytechnique Montreal, C.P. 6079, Succ. Centre Ville, Montreal H3C 3A7, Canada

[§]Department of Chemistry "Giacomo Ciamician", Università di Bologna, Via Selmi, 2, Bologna 40126, Italy

Supporting Information

ABSTRACT: The characteristics of the gate electrode have significant effects on the behavior of organic electrochemical transistors (OECTs), which are intensively investigated for applications in the booming field of organic bioelectronics. In this work, high specific surface area activated carbon (AC) was used as gate electrode material in OECTs based on the conducting polymer poly(3,4-ethylenedioxythiophene) (PEDOT) doped with poly(styrenesulfonate) (PSS). We found that the high specific capacitance of the AC gate electrodes leads to high drain-source current modulation in OECTs, while their intrinsic quasi-reference characteristics make unnecessary the presence of an additional reference electrode to monitor the OECT channel potential.

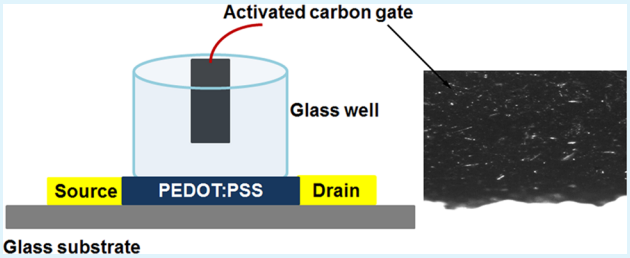

KEYWORDS: *electrochemical transistors, organic electronics, conducting polymers, activated carbon, PEDOT:PSS, electrochemical doping*

INTRODUCTION

The capability of certain organic electronic materials to transport both ionic and electronic charge carriers lays the foundation of organic bioelectronics, where signals are exchanged between organic electronic devices and biological systems.[1] Organic electrochemical transistors (OECTs), first demonstrated in the eighties,[2] are a subclass of organic thin film transistors particularly attractive for applications in bioelectronics. OECTs can be operated at low voltages (below 1 V) in aqueous environments. Simple processing and versatile geometry facilitate OECT fabrication by low-cost solution processing techniques[3] and their integration with microfluidic channels.[4] These properties make OECTs primary candidates for bioelectronic implants,[5] devices to control cell adhesion[6] and viability,[7] chemical and biological sensors,[8] and lab-on-a-chip systems.

OECTs consist of source and drain electrodes and a channel containing a conducting polymer in ionic contact with a gate electrode via an electrolyte solution (Figure 1). The gate-source voltage (V_{gs}) modulates the current flowing in the channel between the drain and source electrodes (I_{ds}). A high current modulation is essential for bioelectronic applications, which require low-voltage operation and high sensitivity.[9]

The majority of OECTs is currently based on thin films of the conducting polymer poly(3,4-ethylenedioxythiophene) (PEDOT) doped with poly(styrenesulfonate) (PSS). PEDOT:PSS films with conductivities in the range of 1000 S cm^{-1}, with good biocompatibility and stability in aqueous environment,[7] are routinely deposited by spin coating of commercially available aqueous suspensions. In the past decade, there has been extensive research on the effects of channel material and electrolyte properties,[10−12] device geometry[13−18] and gate electrode materials[19] on the behavior of OECTs. However, despite these important efforts, the role played by the gate electrode in determining OECT device performance has not been investigated deeply. Gate electrodes for OECTs are typically made of materials such as Pt, Au, Ag, Ag/AgCl and patterned PEDOT:PSS films. Lin et al. investigated the effect of

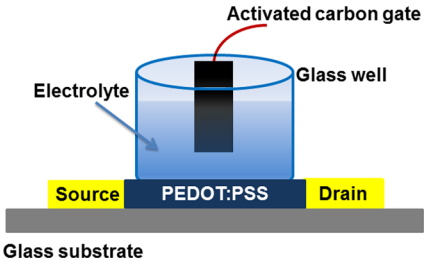

Figure 1. Scheme of the architecture of OECTs using an AC gate electrode and a conducting polymer channel made of PEDOT:PSS.

Received: November 5, 2014
Accepted: December 16, 2014
Published: December 16, 2014

DOI: 10.1021/am507708c
ACS Appl. Mater. Interfaces 2015, 7, 969−973

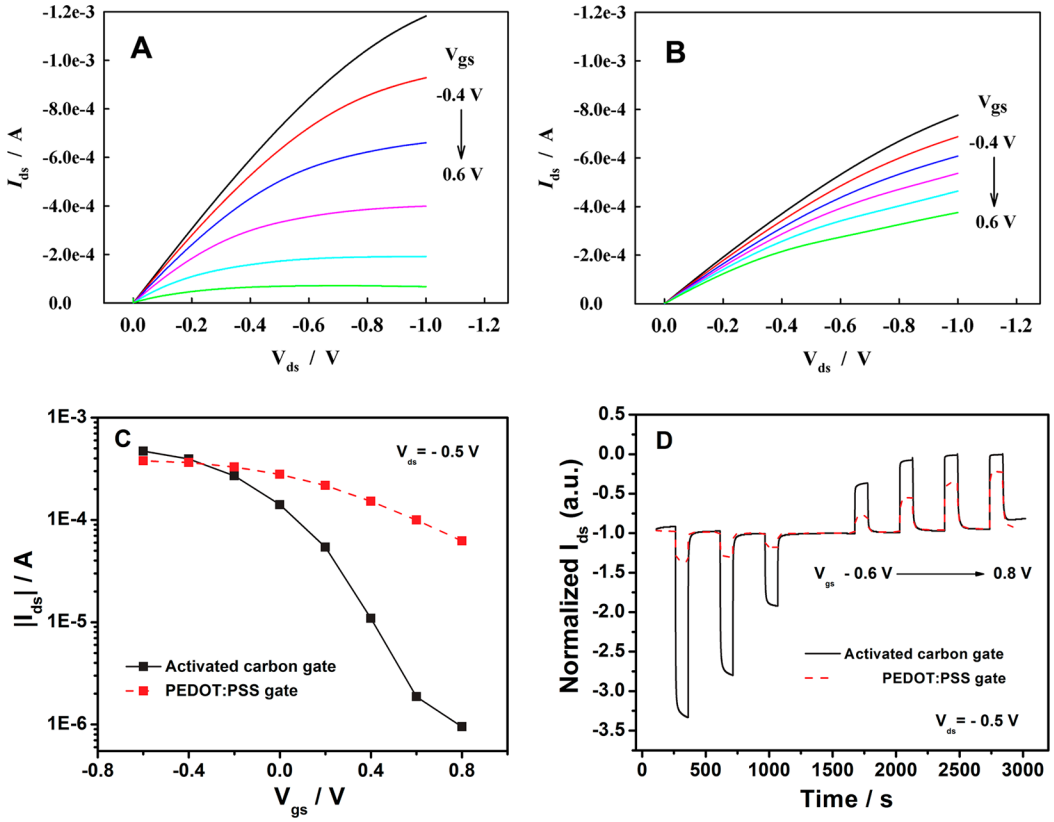

Figure 2. Characteristics of PEDOT:PSS based OECTs using AC and PEDOT:PSS gate electrodes, employing an aqueous solution of NaCl (0.01 M) as the electrolyte. Typical output characteristics obtained with an AC (A) or a PEDOT:PSS gate electrode (B). The V_{ds} scan rate is 5 mV s^{-1} and V_{gs} is varied from −0.4 to +0.6 V in steps of 0.2 V. Transfer characteristics (C) of PEDOT:PSS OECTs using an AC (black line) and a PEDOT:PSS gate electrode (red line) at V_{ds}= −0.5 V and −0.6 V ≤ V_{gs} ≤ 0.8 V. Transient (I_{ds} vs time) responses (D) normalized with respect to the current at V_g= 0 V of OECTs using AC (black solid line) and PEDOT:PSS (red dashed line) gate electrodes at V_{ds}= −0.5 V. From left to right, V_{gs} is pulsed from 0 to −0.6, −0.4, −0.2, +0.2, +0.4, +0.6 and +0.8 V with a pulse duration of 100 s.

the geometric area of the gate electrode (a Pt wire) on the characteristics of an OECT based on a polyacetylene ionomer, and found that the transistor current modulation increases upon increase of the capacitance of the gate electrode.[20] Cicoira et al. studied the response of PEDOT:PSS-based OECTs with Pt and Ag gate electrodes in halide electrolytes and demonstrated that Ag leads to larger current modulation than Pt upon application of the same V_{gs}.[19] This effect was attributed to a Faradaic reaction between Ag and the halide electrolyte.

Activated carbon (AC) is a material of high interest for gate electrodes in OECTs because of its very large specific surface area (about 1000−2000 m^2 g^{-1}),[21] which results in a high specific double-layer capacitance and a high electrostatic charge storage capacity. These properties explain the wide use of AC in double-layer supercapacitors.[21] The use of high specific surface area AC gate electrodes in OECTs is expected to enable to counterbalance the charge required to dedope/dope the channel within a relatively narrow electrode potential excursion, by a fast and highly reversible electrostatic process. This would make possible the use of AC gates as quasi-reference electrodes, dramatically simplifying the device structure. Moreover, the absence of undesired Faradaic (redox) processes at the AC electrode/electrolyte interface would be beneficial for device stability.[22] Along this line, Sayago et al. recently demonstrated that an AC gate electrode enables low-voltage operation in ionic liquid-gated organic transistors based on MEH-PPV semiconducting polymer channels.[23]

In this letter, we investigate OECTs based on PEDOT:PSS using AC gate electrodes. We demonstrate that OECTs with AC gate electrodes show large current modulations and do not require the presence of an additional reference electrode to monitor the channel potential. This behavior is attributed to the high double-layer capacitance of the AC electrode and to its intrinsic property to act as a quasi-reference.

EXPERIMENTAL SECTION

The OECT device architecture used in this work is shown in Figure 1. OECTs based on PEDOT:PSS were patterned following a procedure described in the literature (see the Supporting Information).[17,24] Conducting polymer films (with a thickness of about 200 nm) were deposited by spin coating of a mixture containing a PEDOT:PSS suspension (Hareus Clevios PH 1000), ethylene glycol, dodecyl benzensulfonic acid (DBSA) and (3-glycidyloxypropyl)-trimethoxysilane (GOPS). The OECT channel (geometric area of about 12 mm^2) was defined by the contact region between the PEDOT:PSS film and the electrolyte (0.01 M aqueous solution of NaCl), confined into a glass well. AC gate electrodes were obtained by drop casting about 80 μL of a suspension of AC (PICACHEM BP9, 28 mg mL^{-1}) and Nafion (2.4 mg mL^{-1}) in isopropanol, on stripes of carbon fiber paper (Spectracorp 2050, 10 mils). The channels and gate electrodes (both AC and PEDOT:PSS) of the OECTs studied in this work have a similar geometric area of ∼12 mm^2.

RESULTS AND DISCUSSION

The typical output characteristics of PEDOT:PSS OECTs using AC gate electrodes are shown in Figure 2A and compared

DOI: 10.1021/am507708c
ACS Appl. Mater. Interfaces 2015, 7, 969−973

to those of OECTs with planar PEDOT:PSS gate electrodes (whose structure is shown in the Supporting Information, Figure S1) in Figure 2B. At a given V_{gs}, OECTs using AC gate electrodes exhibit a larger I_{ds} modulation with respect to those using PEDOT:PSS. As an example, at V_{ds}= −0.4 V, upon variation of V_{gs} from −0.4 to +0.6 V, the I_{ds} of OECTs using AC varies by about a factor of 10, while that of the devices using PEDOT:PSS gate electrodes varies by about a factor of 3. Furthermore, the use of AC gate electrodes permits the saturation regime to be achieved at lower V_{ds}. For instance, at V_{gs} = +0.6 V, devices using AC gates saturate at $V_{ds} \approx -0.2$ V, whereas devices using PEDOT:PSS gates do not show saturation even at higher $|V_{ds}|$. The transfer (Figure 2C) and transient (I_{ds} vs time, Figure 2D) characteristics further confirm that a higher I_{ds} modulation is achieved by using AC gate electrodes. In the transfer curves (V_{ds}= −0.5 V and $-0.6 \leq V_{gs} \leq 0.8$ V), the decrease of I_{ds} with V_{gs} is steeper for OECTs with an AC gate electrode compared to those with a PEDOT:PSS gate, which results in a higher ON/OFF ratio (∼500 for OECTs with AC gate compared to ∼15 for OECTs with PEDOT:PSS). The transient characteristics reveal that, for a given V_{gs}, the steady-state value of $|I_{ds}|$ of OECTs with an AC gate (Figure 2D, black solid line) is significantly lower than that of OECTs with a PEDOT:PSS gate (Figure 2D, red dashed line) featuring the same geometric area. We postulate that the low current modulation and the fact that no current saturation is achieved in the output curves in our devices with PEDOT:PSS gates is likely due to the small gate/channel geometric area ratio. Indeed, it has been shown that OECTs with PEDOT:PSS gates can reach current modulations of 1000 and beyond and very efficient saturation, provided that the geometric area of the gate electrode is at least ten times larger than that of the channel.[25] The use of AC gates permits to circumvent such requirement. However, AC gates that feature higher specific areas than PEDOT:PSS may result in relatively high gate currents. Therefore, the AC gate area and mass loading need to be properly optimized to reduce gate currents (Figure S2, Supporting Information) keeping high current modulations (Figure S3, Supporting Information).

The PEDOT:PSS channel of an OECT is dedoped/doped by a Faradaic process, hence its doping level and electronic properties (e.g., electrical conductivity) depend on its electrochemical potential, commonly expressed vs a reference electrode (RE). To shed light onto the different behaviors of devices using AC and PEDOT:PSS gate electrodes, we performed a cyclic voltammetry (CV) study. In all our experiments, a PEDOT:PSS film acted as the working electrode (WE). Initially, a CV scan was carried out using a Pt wire as the counter electrode (CE) and a saturated calomel electrode (SCE) as the RE, to identify the oxidation and reduction peaks of the PEDOT:PSS film. The voltammogram (Figure 3A, solid black curve) shows that such redox peaks are located at about −0.65 V vs SCE (reduction) and −0.35 V vs SCE (oxidation), in agreement with previous publications.[26,27] The CV also reveals that (i) at 0.5 V vs RE, the PEDOT:PSS channel is in a fully doped state, whereas it is dedoped at potentials lower than −0.6 V vs RE; (ii) the WE potential should be kept below 0.6 V vs RE, to prevent overoxidation of PEDOT:PSS. A similar voltammetric response is obtained when the SCE RE is replaced by an AC electrode (Figure 3, dashed red curve), thus indicating that AC can be used as a quasi-reference, with a potential close to that of the SCE.[28,29] To mimic the I_{gs} vs V_{gs} electrochemical response of a PEDOT:PSS OECT channel

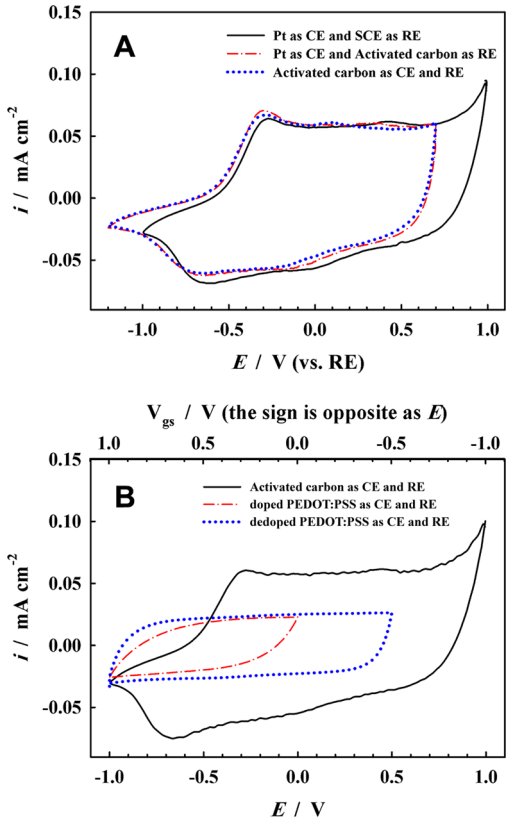

Figure 3. Cyclic voltammograms of various electrochemical cells where the electrolyte is a 0.01 M aqueous solution of NaCl, a doped (pristine) PEDOT:PSS film acts as the working electrode (WE) and different counter electrodes (CE) and reference electrodes (RE) are compared. (A) Three-electrode configuration with a Pt wire CE and a saturated calomel electrode (SCE) RE (black solid line), three-electrode configuration with a Pt wire CE and an AC electrode RE (red dashed curve), two-electrode configuration with an AC electrode acting as CE and RE (blue dotted curve). (B) Two-electrode configuration with an AC electrode (black solid curve) or a doped (pristine) PEDOT:PSS film (red dashed curve) or a dedoped PEDOT:PSS (blue dotted curve) acting simultaneously as CE and RE. The CV scan rate is 50 mV s^{-1}. The top *x*-axis indicates the corresponding V_{gs} in OECTs.

modulated by an AC gate electrode, we performed CVs in a two-electrode configuration, with an AC electrode acting both as the CE and the RE (Figure 3A, dotted blue curve). Remarkably, also in this configuration, the voltammetric response almost overlaps with that obtained in a three electrode configuration using the Pt CE and the SCE RE. This result can be understood taking into account that the current measured during the CV is related to the total capacitance of the two-electrode cell (C), which corresponds to the capacitances of the PEDOT:PSS WE (C_{WE}) and the AC CE (C_{CE}) connected in series, i.e., $C^{-1} = C_{WE}^{-1} + C_{CE}^{-1}$. Because the AC CE has a high-specific surface area and a high-specific capacitance (80 F g^{-1}),[23] in our cell $C_{CE} \gg C_{WE}$, and $C \cong C_{WE}$. This means that the cell current is mainly determined by the response of the PEDOT:PSS WE. Furthermore, the high specific capacitance of the AC CE also permits to keep the potential excursion of the CE within a few tenths of mV during PEDOT:PSS doping/dedoping (the capacitance, C, the charge, Q and the electrode potential excursion, ΔV, are indeed related by $C = Q/\Delta V$). The overlap of the CV curves in Figure 3A

DOI: 10.1021/am507708c
ACS Appl. Mater. Interfaces 2015, 7, 969−973

indicates that the AC electrode is able to effectively dedope/dope the PEDOT:PSS channel, while acting simultaneously as a quasi-reference electrode. When the CV is performed in a two-electrode configuration (Figure 3A, dotted blue curve), the potential applied between the WE (PEDOT:PSS) and the AC quasi-RE corresponds to $-V_{gs}$ in PEDOT:PSS OECTs making use of an AC gate electrode. Therefore, our results indicate that a V_{gs} range between −0.4 to +0.6 V enables to safely and gradually switch the OECT from the ON to the OFF state.

The advantage of using AC gate electrodes in OECTs is further highlighted in Figure 3B, which shows CVs carried out in a two-electrode configuration using AC (black solid curve), doped PEDOT:PSS (red dashed curve) and dedoped PEDOT:PSS (blue dotted curve) as both CE and RE. The most important features of these voltammograms are the following: (i) when PEDOT:PSS films are used as CE and RE, the CVs show no redox peaks within the applied potential range and the current is much lower than that obtained with AC; (ii) to achieve a good cycling efficiency, the cell voltage potential range needs to be kept between −1 and 0 V for doped PEDOT:PSS and between −1 and +0.5 V for dedoped PEDOT:PSS. These results can be explained taking into account that in symmetrical PEDOT:PSS two-electrode cells, the WE and the CE are made of the same material and have a similar geometric area, therefore $C_{WE} \cong C_{CE}$. As a consequence (as $C^{-1} = C_{WE}{}^{-1} + C_{CE}{}^{-1}$), the current is also significantly affected by the response of the CE. According to $C = Q/\Delta V$, the potential excursion (ΔV) of the PEDOT:PSS CE (i.e., of the gate in the OECT) is not negligible and the application of a V_{gs} bias in OECTs with PEDOT:PSS gate electrodes results in an almost equal variation of both the channel and gate electrode potentials. This means that in OECTs where PEDOT:PSS is used as the gate electrode, dedoping (reduction) of the channel is inevitably accompanied by an overdoping (overoxidation) of the gate electrode and V_{gs} does not correspond to the OECT channel potential vs a RE. In a symmetrical two-electrode cell with PEDOT:PSS WE and CE, both in the doped (pristine) state, the initial cell voltage is 0 V (i.e., both the electrodes are at ∼0.5 V vs SCE). Application of a cell voltage of −1 V (corresponding to V_{gs} = 1.0 V in the OECT) would result in a potential excursion of both electrodes of ±0.5 V, with the WE being dedoped down to ∼0 V vs SCE (calculated as ∼0.5 V (vs SCE (initial potential) − 0.5 V (potential excursion)) and the CE being further doped up to 1.0 V vs SCE (∼0.5 V (vs SCE, initial potential) + 0.5 V (potential excursion)), which is well beyond the anodic limit potential for polymer doping. This explains why in Figure 3B (red dashed curve) a good cycling efficiency is achieved only by keeping the cell voltage within 0 and −1 V (corresponding to $0 \leq V_{gs} \leq +1$ V in the OECT). In this case, V_{gs} does not give a precise indication of the OECT channel potential vs a RE, and the gate overdoping has a negative impact on the device stability. In principle, overdoping of the PEDOT:PSS CE can be avoided by dedoping it before use. In a two-electrode cell assembled with doped (pristine) polymer WE (at ∼0.5 V vs SCE) and dedoped CE (at least −0.6 V vs SCE), application of a cell voltage of −1.0 V would again shift the potentials of both the WE and the CE by ∼±0.5 V, bringing the WE at ∼0 V vs SCE (see above) and the CE at ∼−0.1 vs SCE (∼−0.6 V (vs SCE, initial potential) + 0.5 V (potential excursion)), which is within a safe electrode potential window for both polymer electroactivity and electrolyte stability. Indeed, the CV in Figure 3B (blue dotted curve) shows that a dedoped CE allows cycling in a wider cell voltage range with respect to a doped (pristine) PEDOT:PSS CE (red dashed curve). However, the low voltammetric currents indicate that, even in this case, the polymer gate charge storage capability would limit the channel doping/dedoping in an OECT with a PEDOT:PSS gate. The polymer CE changes potential upon cycling and cannot be used as RE. This means that even dedoped PEDOT:PSS gates cannot lead to the same OECTs modulation as AC gates. Furthermore, the dedoped PEDOT:PSS CE would have a conductivity that changes upon the OECT operation, which in turn would affect how the potential is distributed upon applying the gate voltage.

CONCLUSIONS

In conclusion, we investigated PEDOT:PSS OECTs using high specific surface area AC gate electrodes. The use of AC gate electrodes leads to higher current modulations, at low voltage, compared to PEDOT:PSS gate electrodes of comparable geometric area. Cyclic voltammetry studies, where PEDOT:PSS is used as the WE and AC is used as the RE and CE, show that high double-layer capacitance and absence of Faradaic processes permit the development of OECTs where the channel potential is uniquely determined by the applied gate bias. Processing and integrating AC electrodes into in-plane, flexible device architectures[30] could represent a step forward in the search of new electrode materials for OECTs to be used in biosensors and other bioelectronics devices.

ASSOCIATED CONTENT

Supporting Information

Details for the fabrication of the OECT devices, preparation of the AC electrodes and electrochemical measurements. Scheme demonstrating the architecture of OECTs using PEDOT:PSS gate electrodes. Gate/source current characteristics of OECTs using AC and PEDOT:PSS gate electrodes and current modulations with different AC electrode areas. This material is available free of charge via the Internet at http://pubs.acs.org.

AUTHOR INFORMATION

Corresponding Author

*F. Cicoira. Tel.: 1-514-340-4711 ext. 2580. Fax: 1-514-340-2990. E-mail: Fabio.cicoira@polymtl.ca.

Author Contributions

⊥H.T., P.K. and S.Z. equally contributed to this work. The paper was written through contributions of all authors. All authors have given approval to the final version of the paper.

Funding

Natural Sciences and Engineering Research Council of Canada (NSERC), Università di Bologna, Polytechnique Montreal CMC microsystems.

Notes

The authors declare no competing financial interest.

ACKNOWLEDGMENTS

The authors are grateful to Daniel Pilon for technical support. This research is supported by NSERC Discovery Grants (FC, CS and GDC). F.C. acknowledges Polytechnique Montreal for a Startup Grant. S.Z. and Z.Y. acknowledges the Government of Canada for a Vanier Canada Scholarship. H.T. and P.K. acknowledge the Groupe de Recherche en Sciences et Technologies Biomédicales for partial salary support. F.S. acknowledges financial support by Università di Bologna

DOI: 10.1021/am507708c
ACS Appl. Mater. Interfaces 2015, 7, 969−973

(researcher mobility program, Italian-Canadian cooperation agreement). This work is supported by CMC Microsystems through the programs CMC MNT and CMC Solutions.

REFERENCES

(1) Gomez-Carretero, S.; Kjäll, P. Medical Applications of Organic Bioelectronics. In *Organic Electronics: Emerging Concepts and Technologies*; Cicoira, F., Santato, C., Eds.; Wiley-VCH Verlag GmbH & Co. KGaA: Weinheim, 2013; Chapter 3, pp 69−89.
(2) White, H. S.; Kittlesen, G. P.; Wrighton, M. S. Chemical Derivatization of an Array of Three Gold Microelectrodes with Polypyrrole: Fabrication of a Molecule-based Transistor. *J. Am. Chem. Soc.* **1984**, *106*, 5375−5377.
(3) Basiricò, L.; Cosseddu, P.; Scidà, A.; Fraboni, B.; Malliaras, G. G.; Bonfiglio, A. Electrical Characteristics of Ink-Jet Printed, All-Polymer Electrochemical Transistors. *Org. Electron.* **2012**, *13*, 244−248.
(4) Yang, S. Y.; DeFranco, J. A.; Sylvester, Y. A.; Gobert, T. J.; Macaya, D. J.; Owens, R. M.; Malliaras, G. G. Integration of a Surface-Directed Microfluidic System with an Organic Electrochemical Transistor Array for Multi-Analyte Biosensors. *Lab Chip* **2009**, *9*, 704−708.
(5) Owens, R. M.; Malliaras, G. G. Organic Electronics at the Interface with Biology. *MRS Bull.* **2010**, *35*, 449−456.
(6) Bolin, M. H.; Svennersten, K.; Nilsson, D.; Sawatdee, A.; Jager, E. W. H.; Richter-Dahlfors, A.; Berggren, M. Active Control of Epithelial Cell-Density Gradients Grown along the Channel of an Organic Electrochemical Transistor. *Adv. Mater.* **2009**, *21*, 4379−4382.
(7) Lin, P.; Yan, F.; Yu, J.; Chan, H. L. W.; Yang, M. The Application of Organic Electrochemical Transistors in Cell-based Biosensors. *Adv. Mater.* **2010**, *22*, 3655−3660.
(8) Lin, P.; Yan, F. Organic Thin-Film Transistors for Chemical and Biological Sensing. *Adv. Mater.* **2012**, *24*, 34−51.
(9) Khodagholy, D.; Rivnay, J.; Sessolo, M.; Gurfinkel, M.; Leleux, P.; Jimison, L. H.; Stavrinidou, E.; Herve, T.; Sanaur, S.; Owens, R. M.; Malliaras, G. G. High Transconductance Organic Electrochemical Transistors. *Nat. Commun.* **2013**, *4*, 2133−2138.
(10) Bubnova, O.; Berggren, M.; Crispin, X. Tuning the Thermoelectric Properties of Conducting Polymers in an Electrochemical Transistor. *J. Am. Chem. Soc.* **2012**, *134*, 16456−16459.
(11) Alam, M. M.; Wang, J.; Guo, Y.; Lee, S. P.; Tseng, H.-R. Electrolyte-Gated Transistors Based on Conducting Polymer Nanowire Junction Arrays. *J. Phys. Chem. B* **2005**, *109*, 12777−12784.
(12) Tarabella, G.; Nanda, G.; Villani, M.; Coppedé, N.; Mosca, R.; Malliaras, G. G.; Santato, C.; Iannotta, S.; Cicoira, F. Organic Electrochemical Transistors Monitoring Micelle Formation. *Chem. Sci.* **2012**, *3*, 3432−3435.
(13) Chao, S.; Wrighton, M. S. Solid-State Microelectrochemistry: Electrical Characteristics of a Solid-State Microelectrochemical Transistor Based on Poly(3-methylthiophene). *J. Am. Chem. Soc.* **1987**, *109*, 2197−2199.
(14) Jones, E. T. T.; Chyan, O. M.; Wrighton, M. S. Preparation and Characterization of Molecule-based Transistors with a 50-Nanometer Source-Drain Separation with Use of Shadow Deposition Techniques. Toward Faster, More Sensitive Molecule-based Devices. *J. Am. Chem. Soc.* **1987**, *109*, 5526−5528.
(15) Berggren, M.; Forchheimer, R.; Bobacka, J.; Svensson, P. O.; Nilsson, D.; Larsson, O.; Ivaska, A. PEDOT:PSS-based Electrochemical Transistors for Ion-to-Electron Transduction and Sensor Signal Amplification. In *Organic Semiconductors in Sensor Applications*; Bernards, D., Malliaras, G., Owens, R., Eds.; Springer: Berlin/Heidelberg, 2008; Chapter 9, pp 263−280.
(16) Bernards, D. A.; Malliaras, G. G. Steady-State and Transient Behavior of Organic Electrochemical Transistors. *Adv. Funct. Mater.* **2007**, *17*, 3538−3544.
(17) Cicoira, F.; Sessolo, M.; Yaghmazadeh, O.; DeFranco, J. A.; Yang, S. Y.; Malliaras, G. G. Influence of Device Geometry on Sensor Characteristics of Planar Organic Electrochemical Transistors. *Adv. Mater.* **2010**, *22*, 1012−1016.
(18) Yaghmazadeh, O.; Cicoira, F.; Bernards, D. A.; Yang, S. Y.; Bonnassieux, Y.; Malliaras, G. G. Optimization of Organic Electrochemical Transistors for Sensor Applications. *J. Polym. Sci., Part B: Polym. Phys.* **2011**, *49*, 34−39.
(19) Tarabella, G.; Santato, C.; Yang, S. Y.; Iannotta, S.; Malliaras, G. G.; Cicoira, F. Effect of the Gate Electrode on the Response of Organic Electrochemical Transistors. *Appl. Phys. Lett.* **2010**, *97*, 123304.
(20) Lin, F.; Lonergan, M. C. Gate Electrode Processes in an Electrolyte-Gated Transistor: Non-Faradaically versus Faradaically Coupled Conductivity Modulation of a Polyacetylene Ionomer. *Appl. Phys. Lett.* **2006**, *88*, 133507.
(21) Conway, B. E. *Electrochemical Supercapacitors: Scientific Fundamentals and Technological Applications*; Springer US: New York, 1999.
(22) Inzelt, G. Pseudo-Reference Electrodes. In *Handbook of Reference Electrodes*; Inzelt, G., Lewenstam, A., Scholz, F., Eds.; Springer: Berlin/Heidelberg, 2013; Chapter 14, pp 331−332.
(23) Sayago, J.; Soavi, F.; Sivalingam, Y.; Cicoira, F.; Santato, C. Low Voltage Electrolyte-Gated Organic Transistors Making Use of High Surface Area Activated Carbon Gate Electrodes. *J. Mater. Chem. C* **2014**, *2*, 5690−5694.
(24) Rivnay, J.; Leleux, P.; Sessolo, M.; Khodagholy, D.; Hervé, T.; Fiocchi, M.; Malliaras, G. G. Organic Electrochemical Transistors with Maximum Transconductance at Zero Gate Bias. *Adv. Mater.* **2013**, *25*, 7010−7014.
(25) Andersson, P.; Forchheimer, R.; Tehrani, P.; Berggren, M. Printable All-Organic Electrochromic Active-Matrix Displays. *Adv. Funct. Mater.* **2007**, *17*, 3074−3082.
(26) Demelas, M.; Scavetta, E.; Basiricò, L.; Rogani, R.; Bonfiglio, A. A Deeper Insight into the Operation Regime of All-Polymeric Electrochemical Transistors. *Appl. Phys. Lett.* **2013**, *102*, 193301.
(27) Laforgue, A.; Robitaille, L. Production of Conductive Pedot Nanofibers by the Combination of Electrospinning and Vapor-Phase Polymerization. *Macromolecules* **2010**, *43*, 4194−4200.
(28) Weigarth, D.; Foelske-Schmitz, A.; Wokaun, A.; Kötz, R. PTFE Bound Activated Carbon—A Quasi-Reference Electrode for Ionic Liquids. *Electrochem. Commun.* **2012**, *18*, 116−118.
(29) Ruch, P. W.; Cericola, D.; Hahn, M.; Kötz, R.; Wokaun, A. On the Use of Activated Carbon as a Quasi-Reference Electrode in Non-Aqueous Electrolyte Solutions. *J. Electroanal. Chem.* **2009**, *636*, 128−131.
(30) Beidaghi, M.; Gogotsi, Y. Capacitive Energy Storage in Micro-Scale Devices: Recent Advances in Design and Fabrication of Microsupercapacitors. *Energy Environ. Sci.* **2014**, *7*, 867.

DOI: 10.1021/am507708c
ACS Appl. Mater. Interfaces 2015, 7, 969−973